

Micro Scribing of Copper and Aluminum Thin Films in Air and Water Using Pulsed Nd³⁺:YAG Laser

Srinagalakshmi Nammi¹, Ankit K Jain¹, Nilesh J Vasa¹, G Balaganesan², Anil C Mathur³

¹ Department of Engineering Design, Indian Institute of Technology Madras, Chennai 600036, India
Email: snl.nammi@gmail.com

² Department of Mechanical Engineering, Indian Institute of Madras, Chennai 600036, India

³ Scientist, Antenna Mechanical Design Division, Indian Space Research Organization, Ahmedabad 380015, India

Micro scribing of copper and aluminum thin films in air and underwater using Q-switched Nd³⁺:YAG laser has been described. Influence of de-ionized (DI) water level on the scribed micro channel depth and width has been studied for different wavelengths. Scribing was done by maintaining different levels of DI water at 1mm, 2 mm, 3 mm, 5 mm and 10mm. At 1 mm DI water level and laser pulse energy of 3 mJ, maximum ablation depth of 105 μm was achieved with both 355 nm and 532 nm wavelength for aluminum. Further, the depth achieved in DI water was 6 times greater than that in air for aluminum. On the other hand, for copper film, the depth attained with the laser ablation in DI water was 7 μm as compared to 4 μm in air for 1064 nm wavelength and 40 mJ of energy. In case of 355 nm and 532 nm the depth attained in air was higher than in DI water for copper. As the DI water level was increased, the depth reduced for both aluminum and copper. A comparative study of the results obtained in both underwater and air media revealed that aluminum can be machined more potently in DI water than in air. Further, theoretical modeling of the laser-material interaction in air as ambience has been discussed to estimate the recession rate by incorporating the laser ablation temperature measured using the laser induced breakdown spectroscopy technique.

DOI: 10.2961/jlmn.2016.01.0009

Keywords: laser scribing, under water scribing, thin films, parabolic reflector, laser micro machining

1. Introduction

In communication satellites, aluminum/copper films coated with polyimide substrate are used in parabolic RF antennas. The reflector surface has evenly spaced conductive grids with size ranging in the order of microns. The size and shape of the grids influence the effective functioning of the reflector. Conventionally, the conductive grids on the polyimide substrate are fabricated by mechanical methods that involve cutting of thin metal sheets into finer strips and pasting them in parallel lines on the surface of the reflector. Research is widely carried out in search of precise and reliable fabrication processes for producing these conductive grids.

Pulsed laser ablation (PLA) has been widely studied in the past as an effective method for the ablation of thin metal films [1]. Removal of material occurs due to the interaction of the intense electromagnetic waves in the laser radiation with the work piece, leading to heating, melting and vaporization of a selective micro volume. In contrast with a conventional machine tool process, laser machining process does not involve tool wear, vibrations and burr formation; material removal depends on the optical and thermal properties of the workpiece [2]. Nano second laser pulse absorbed by the workpiece vaporizes a focused volume of material through heat conduction. The ejected vapour interacts with the incoming laser beam and forms a plasma plume [3]. Depending on the ambient conditions, the plasma plume exerts a recoil pressure, expelling the melt pool that gets redeposited at the edge of the crater or channel [4]. In order to avoid this redeposition of expelled material on the workpiece surface, many techniques are being used that includes high pressure gas/liquid. Laser coupled with high pressure water through total internal reflection shows better surface quality and reduced heat

affected zone when scribing thin brass and stainless steel work pieces [5]. Underwater laser ablation of aluminum is shown as a cost effective drilling process compared to dry ablation, with improvement in the crater shape quality [6]. Metal plates of varying thicknesses have been drilled using Nd³⁺:YAG laser in water and air and the material removal in under water drilling is 10 times more than in air due to the plasma confinement by water [7]. Bubble formation and collapse due to vapourization of water is shown to be an effective method for removal of debris in wet ablation process [8].

Many research groups have reported on under water laser ablation process including only infrared wavelength. However, there is a need to understand the behavior of laser ablation of Al/Cu films for a wide range of laser wavelengths. Laser scribing of reflective materials, such as Cu and Al films has not been studied in detail. Micro machining on thin copper films was performed for three laser wavelengths (355 nm, 532 nm and 1064 nm) and the effect of intensity and processing rate on the surface morphology has been investigated in air [9,10]. Free-electron thermal conductivity is high in these metals and it makes the controlled machining of reflective materials using laser a challenging task. Aluminum has very high reflectivity (approximate 90%) due to multi-valency of the metal that is responsible for high plasma frequency of Al [11]. However, there are very few reports on the same using the ns-pulsed Nd³⁺:YAG laser in particular.

This paper aims at presenting certain results related to under water laser scribing using UV (355 nm), visible (532 nm) and IR (1064 nm) wavelengths of a Q-switched, pulsed Nd³⁺:YAG. The influence of various laser parameters such as laser beam profile, wavelength and ambient condition has been studied to develop laser scribing tech-

niques for manufacturing micro-channels on Al/Cu film deposited on a flexible substrate. Further, the laser induced breakdown spectroscopy (LIBS) technique has been proposed and demonstrated for estimating the plume temperature during the laser scribing of thin films. Theoretical modeling has also been attempted to understand the effect of different wavelengths (355 nm, 532 nm and 1064 nm) on the recession rate and ablation temperature for thin copper sample and the results are discussed.

2. Experiment Studies

2.1 Experimental Setup

A Q-switched Nd³⁺:YAG laser with a pulse width of 6 ns and a repetition rate of 5 Hz was used in this study. The laser beam was directed on to the workpiece using beam alignment optics such as dichroic mirrors and a quartz lens with a focal length of 250 mm as shown in figure 1. Laser scribing was performed on 150 μm thickness Al film and 35 μm thickness Cu films on a 50 μm thick polyimide substrate. Experiments in air medium with the Gaussian laser beam profile were performed by mounting the workpiece on a motorized X-Y stage. On the other hand, experiments in under water medium with de-ionized water were performed by fixing the workpiece in a water beaker placed over the X-Y stage. During LIBS study, the optical emission was collected at an angle of 30° by a lens of focal length 150 mm and was focused onto an optical fiber (core diameter 600 μm, NA 0.39). A spectrometer (UV-VIS2000, Ocean Optics) coupled with the fiber was used for the detection of spectral information. Surface characterization after the scribing process was carried out using a non-contact optical profilometer (Contour GT-I, Bruker) and a scanning electron microscope (Quanta 200, FEG).

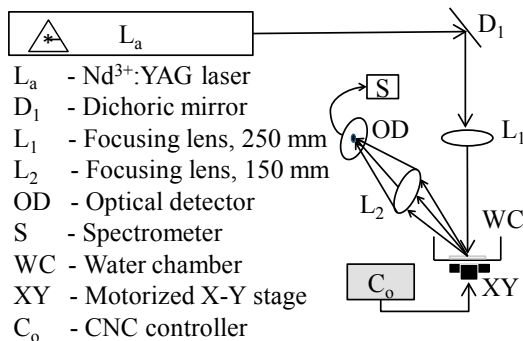


Fig. 1 Schematic of experimental setup used for laser scribing in air and under water

Table 1: Parameters and specifications used in the experiment to study the influence of wavelength and ambience

Parameters	Specifications
Laser used	Nd ³⁺ :YAG ($\lambda=355, 532$ and 1064 nm)
Pulse duration (Frequency)	5 ns (5 Hz)
Cu and Al sample size	20 mm x 20 mm
Focal length	250 mm
Spot size (estimated)	≈ 200 μm
Beam overlap	95%
Ambient condition	Air, DI water (1 -10 mm above the sample)

2.2 Experimental Results

2.2.1 Scribing of copper thin film coated on a polyimide substrate

3D non contact optical profilometer images of micro channels produced under air and water media are shown in figures 2 and 3. A reduction in the redeposition around the scribe edges in underwater laser scribing can be seen in figure 3. The variation in depth of the scribed micro-channels on Cu films, against different laser energy maintained for ablation with three different wavelengths of 355 nm, 532 nm and 1064 nm and under air and DI water media is shown in figures 4-6. In all the cases, initially, with increase in the laser energy, the ablation depth increased but at higher levels of laser energy, either the increase in depth was saturated or the overall depth was decreased. For 95% overlap of the laser spot diameter and 45 mJ of energy, 532 nm wavelength laser resulted in a depth of ~ 21 μm compared to ~ 12 μm using 355 nm and ~ 5 μm using 1064 nm. From figures 4 and 5 it could be seen that for energy less than 25 mJ both 355 nm and 532 nm resulted in same depth, as the laser energy increases depth reduced for 355 nm wavelength compared to 532 nm. Under water scribing of Cu thin films show a reduction in the redeposition of the ablated material as seen in figure 3, but the channel depth achieved was less compared to air for 532 and 355 nm wavelengths as seen from figures 4 and 5. However, for 1064 nm Cu shows an opposite trend; the micro channel depth for underwater scribing was ~ 7 μm compared to ~ 4 μm produced in air. Increasing the height of DI water level above the workpiece has reduced the depth achieved. The change in width of the channel with respect to increase in laser energy was observed to be in few tens of microns.

2.2.2 Scribing of aluminum thin film

Figures 7-9 show the variation in depth of the scribed micro-channels on Al films, against different laser energies ablated with three different wavelengths of 355 nm, 532 nm and 1064 nm in air and water mediums. It was observed that the ablation depth of micro channels produced in Al through underwater laser scribing was 6 times greater compared to the depth achieved in air for all the 3 wavelengths. It was observed that a depth of ~ 100 μm was achieved using both 355 nm and 532 nm with 4 mJ of energy and, 80 μm depth was achieved using 1064 nm, while maintaining the same laser energy. The depth achieved for ablation in air medium, using 1064 nm wavelength with 4 mJ of energy was 10 μm which is less compared to the 20 μm depth achieved using 355 nm and 532 nm respectively. The ablation depth in air is seen to be increasing with increasing energy as seen in Figure 7-9, but laser ablation depths achieved in DI water medium tends to increase and start to reduce/ saturate after ~ 5 mJ energy. Also the ablation depth was reducing as the DI water level above the workpiece increased for all the 3 wavelengths. The width of the micro channels obtained for energies up to 4 mJ was ~ 160 μm and was found to increase to ~ 200 μm for 7 mJ and remained unchanged with further increase of energy. This shows a slight increase in the depth of the channel with increase in energy but then after threshold energy the change in width was negligible for both air and DI water.

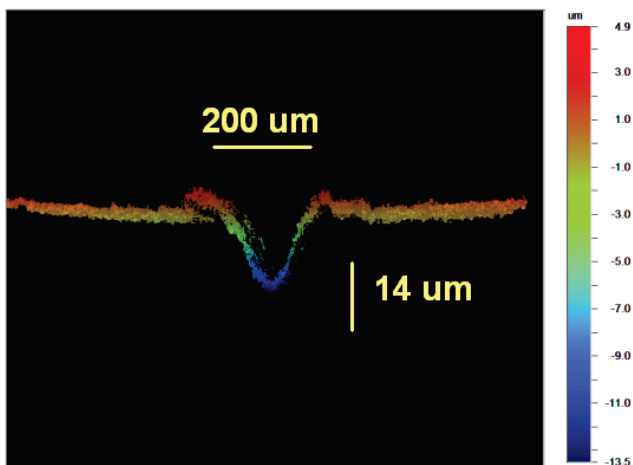


Fig. 2 3D image of the micro channel produced using 532 nm wavelength on Cu thin film coated on a polyimide substrate with 25 mJ energy in air

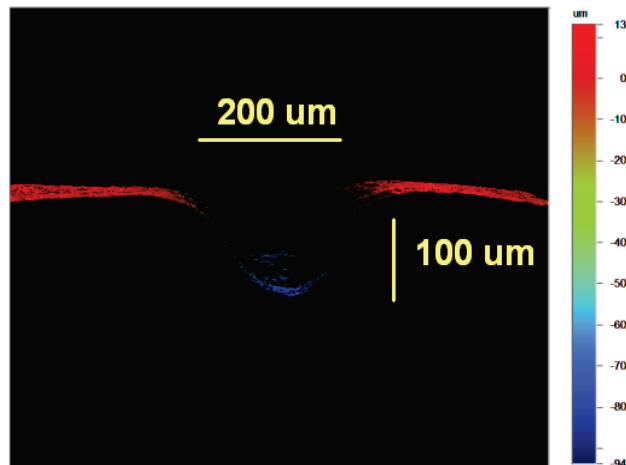


Fig. 3 3D image of the micro channel produced using 532 nm wavelength on Al thin film 5 mJ energy in DI water with 3 mJ energy

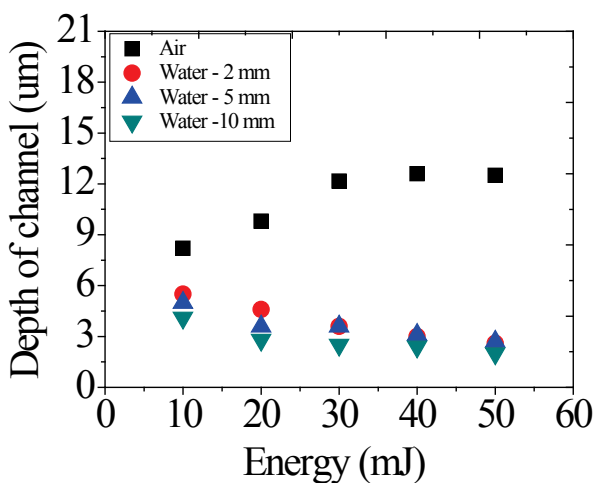


Fig. 4: Change in depth of copper thin film coated on polyimide substrate in air and different DI water levels for 355 nm

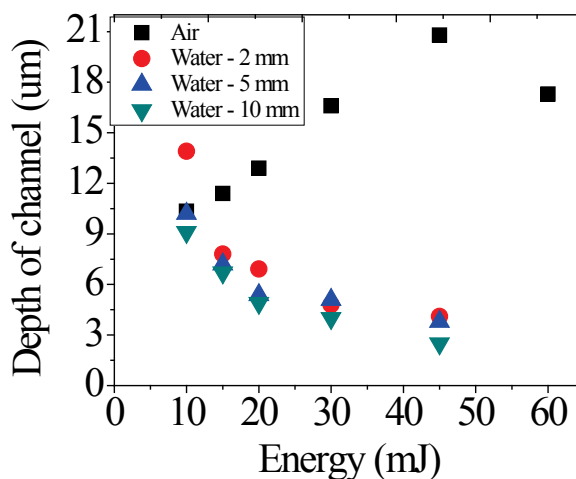


Fig. 5 Change in depth of copper thin film coated on polyimide substrate in air and different DI water levels for 532 nm

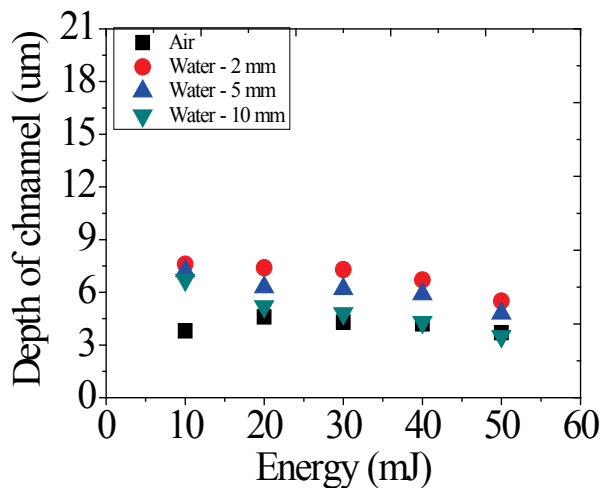


Fig. 6 Change in depth of copper thin film coated on polyimide substrate in air and different DI water levels for 1064 nm

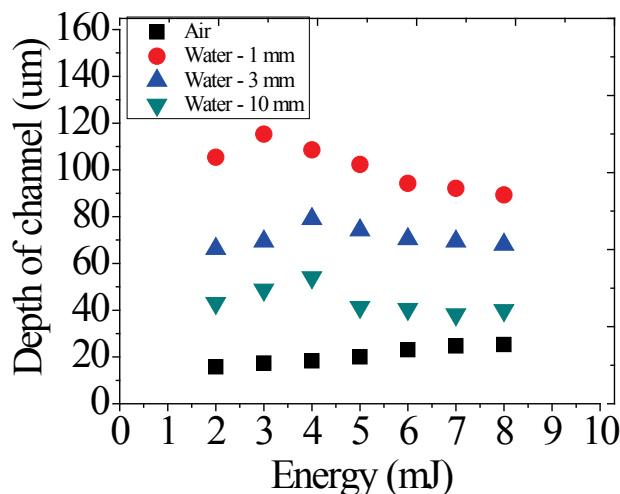


Fig. 7 Change in depth of aluminum thin film in air and different DI water levels for 355 nm

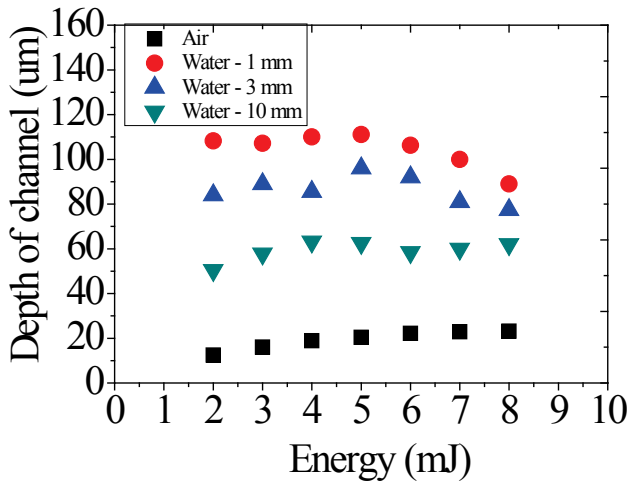


Fig. 8 Change in depth of aluminum thin film in air and different DI water levels for 532 nm

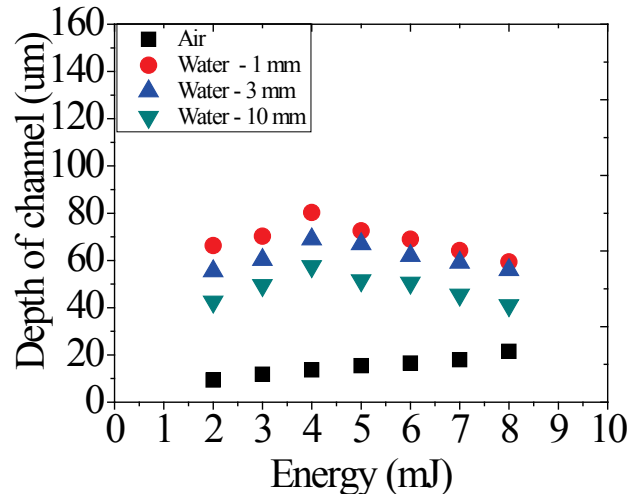


Fig. 9 Change in depth of aluminum thin film in air and different DI water levels for 1064 nm

3. Theory of laser ablation of thin films

In metals, light is absorbed by interaction with electrons. Excited electrons rise to conduction band and collide with lattice phonons, thereby transferring the absorbed energy to the lattice. Since the energy relaxation time is of the order of 10^{-13} s for metals [12], the optical energy can be considered to be converted instantly into heat for ns-pulsed laser ablation. A thermal model of the laser impact on a solid Cu/Al target is developed and studied to understand the phenomenological changes happening during the laser ablation process. Interaction of laser on the target surface increases the temperature at the contact interface, and the target will be able to melt, and even vaporize. The temperature distribution inside the target is calculated by means of the heat conduction equation (1). The absorption length in the target is in the order of 10 nm.

$$\frac{\partial T(x, t)}{\partial t} = \frac{\partial}{\partial x} \left[\left(\frac{k}{\rho C_p} \right) \frac{\partial T(x, t)}{\partial y} \right] + \frac{\alpha}{\rho C_p} I(x, t) \quad (1)$$

where T represents the temperature inside the target, x is the position from the surface; t is the time, k , C_p , ρ and α denotes the thermal conductivity, heat capacity, mass density and absorption coefficient of the target material, respectively. Laser irradiance $I(x, t)$, a function of position and time as represented in equation (2), according to Beer-Lamberts law [12]

$$I(x, t) = I_0(t) \exp(-\alpha x) [1 - \check{R}] \quad (2)$$

where \check{R} is reflectivity and $I_0(t)$ is the laser fluence at time t . When a pulse of laser beam is incident on the target surface, it interacts with the material and the lattice temperature increases accordingly. With the lattice temperature approaching the melting point of the target material, phase change is initiated and the temperature remains almost constant. After the solid to liquid phase transformation, the temperature again tends to increase and as it reaches the boiling point, the material starts to vaporize. The vapor pressure is given by Clausius-Clapeyron equation [12].

$$p_{vap}(T_s) = p_0 \exp \left[\frac{\Delta H_{lv}(T_s - T_b)}{RT_s T_b} \right] \quad (3)$$

where T_s and T_b are the surface temperature and the normal boiling point respectively, pressure p_0 is 100 KPa, ΔH_{lv} is the latent heat of vaporization, and R is the gas constant. The flux of evaporated atoms is obtained from the vapor pressure at the surface temperature by the following equation [12].

$$j_{evap}(T_s) = \frac{A_p(T_s)}{\sqrt{2\pi MRT_s}} \quad (4)$$

where M is the molecular mass of the atoms (kg) and ρ the mass density (kg/m^3). The surface recession rate due to evaporation is calculated from the flux of evaporated atoms using the equation 5.

$$R_{recession} = \frac{dx_{evap}}{dt} = \frac{j_{evap} M}{\rho} \quad (5)$$

3.1 Theoretical modeling Results for Cu thin film

In order to understand the amount of heat conducted into the workpiece during the laser ablation process the temperature and recession rate have been calculated for 355, 532 and 1064 nm laser wavelength using a Gaussian shaped laser beam. Only a single laser pulse is considered for calculating the temperature and recession rate using the parameters tabulated in Table 2. Initially the copper target is considered to be at room temperature and the same is heated using the laser irradiance. In the current model, it is assumed that the absorption coefficient and the thermal conductivity of the target layer drop to zero as soon as the temperature of that particular layer reaches 9000 K. This condition is applied in order to indicate that the material has been removed and the remaining heat energy will propagate to the next layer. The plasma electron temperature is calculated to be 9000 K which is assumed as the temperature at which ablation takes place.

The plasma electron temperature represented in equation (6) is estimated based on Boltzmann-Saha method [13] using the emission spectrum captured using LIBS technique shown in figure 10 [14].

$$T_e = 1.44 \frac{E_2 - E_1}{\ln \left[\frac{I_1 \lambda_1 A_2 g_2}{I_2 \lambda_2 A_1 g_1} \right]} \quad (6)$$

Where T_e is the plasma electron temperature for copper sample E_1 and E_2 are excited energy levels g_1 and g_2 are statistical weights of excited energy levels A_1 and A_2 are the transition probabilities of states I_1 and I_2 are intensity of particular atomic species at λ_1 and λ_2 wavelengths respectively

Table 2 Parameters used in temperature estimation

SNo	λ (nm)	E (cm ⁻¹)	g_k	A_k	I
1	510.5	30783.69	4	2×10^6	20933.7
2	521.8	49942.05	6	7.5×10^7	56388.2

Table 3 Parameters and specifications used in to modeling the influence of wavelength on Cu thin films

Parameters	Specifications
Wavelength	355 nm, 532 nm, 1064 nm
Pulse duration	5 ns
Pulse Fluence	20 J/cm ²
Cu sample size	60 μ m x 10 μ m
Spot size (estimated)	50 μ m
Reflectivity	0.45 (355), 0.65 (532), 0.97 (1064)
Absorption Coefficient	7.1×10^5 cm ⁻¹ (355), 5.8×10^5 cm ⁻¹ (532), 8.6×10^5 cm ⁻¹ (1064)
Copper vapourization temperature	2836 K

4. Discussion

Cu and Al thin films were ablated with three different wavelengths 355 nm, 532 nm and 1064 nm respectively. To find the influence of wavelength and the ambient conditions on the characteristics of the scribed features, depth and width of micro channel are measured using 3D non contact profilometer. It was observed that for both the metals with increase in energy, ablation depth increases but at higher energy, depth of channel remains unchanged. In a study conducted [15], it was found that the shorter wavelength (in the UV region) caused a large absorption of laser energy by the surface and led to a higher temperature rise at the interface leading to a lower threshold fluence value. This is supported by the fact that the surface reflectivity for Cu is 0.45 for 355 nm, 0.62 for 532 nm and 0.97 for 1064 nm, and the absorption coefficient is 7.1×10^5 cm⁻¹ for 355 nm, 6.1×10^5 cm⁻¹ for 532 nm, and 8.1×10^5 cm⁻¹ for 1064 nm [16]. Since the absorption depth is high for 532 nm, it is possible to achieve a greater depth in comparison with 355 nm and 1064 nm for same energy. Moreover, at higher energies the micro channels produced using 355 nm wavelength showed a higher heat affected zone around the channel edges, which is an indication of plasma formation and subsequent heating of the workpiece, which is the cause of reduction in the depth. The formation of plasma above the processing surface can lead to shielding of the work piece surface from the incident beam, thereby preventing the incident beam from coupling to the work piece surface. Previous experimental investigations into the

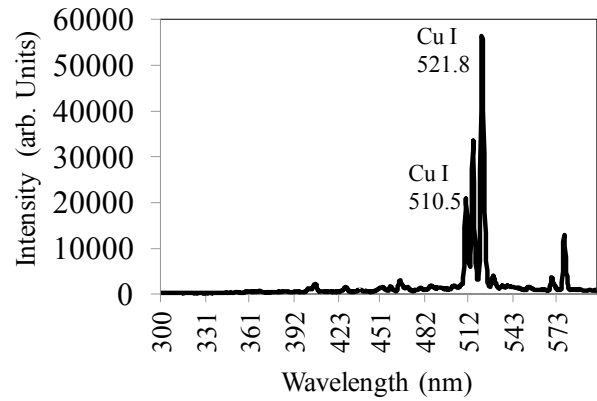


Fig. 10 Optical emission spectra obtained using LIBS technique for copper film coated with polyimide substrate using 15mJ energy

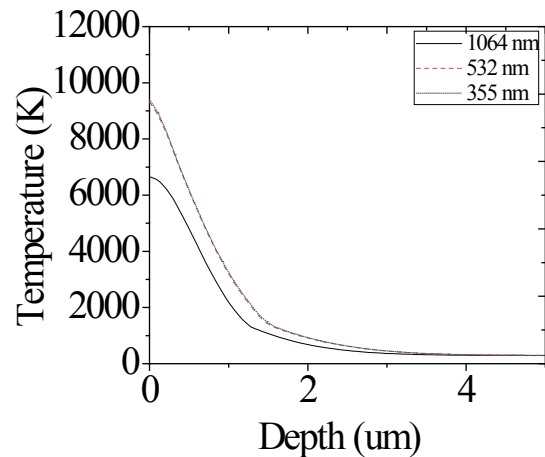


Fig. 11(a) Temperature plot for Cu along the depth profile for 3 different wavelengths at 20 J/cm² fluence

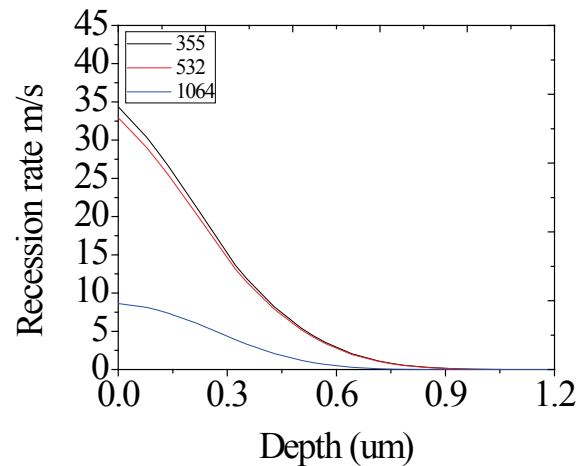


Fig. 11(b) Recession rate for Cu along the depth profile for 3 different wavelengths: 1064 nm, 532 nm and 355 nm

interaction of a short wavelength laser with various metals and ceramics have shown that the formation of plasma over the work piece surface can lead to decoupling of the incident beam from the work piece surface [8]. In underwater scribing, as the DI water level above the work piece decreases, ablation rate increases resulting in increased depth of the scribed channel.

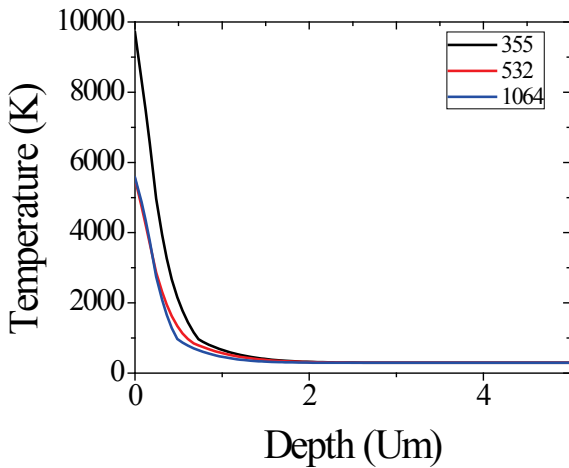


Fig 12: Temperature plot for Al along the depth profile for 3 different wavelengths at 5 J/cm^2 fluence

For a DI water level $h = 1 \text{ mm}$, depth of micro channel is maximum. Increasing the DI water height leads to absorption of laser energy by the medium especially for 1064 nm, causing a reduction in the available energy at the target. No re-deposition at the edges is observed when micro scribing is done in DI water medium. If the work piece is covered with a DI water layer, the plasma is confined and its expansion is delayed. Therefore, the induced pressure is 4 to 10 times greater than the corresponding one obtained in air medium and the shock wave duration is 2–3 times longer than in the air regime at the same power density [17]. This results in higher material removal rates resulting in high ablation depth. Copper has less reflectivity at shorter wavelengths; reflectivity also plays a role in underwater laser scribing. The sudden increase in temperature due to the laser pulse induces shock waves caused by the cavitation bubbles that expand and collapse forming a high pressure liquid jet. These shock waves are reflected by the work piece and are reflected back from the air-DI water interface and increase the impact on the work piece. Because of high reflectivity of Al, depth in DI water is higher for all wavelengths, whereas Cu has lesser reflectivity at shorter wavelength which explains the reduced depth. The micro channel depth is increasing for Al with energy but after certain value of laser energy (5 mJ-6 mJ) depth decreases. It is because of the parasitic plasma occurring in confining DI water. It has been reported that above a 10 GW/cm^2 laser intensity threshold, a saturation of the peak pressure is shown to occur while the shock wave duration is reduced by parasitic plasma occurring in the confining DI water [17]. This phenomenon occurs at the surface of the DI water rather than within the water volume which leads to absorption of the incident laser energy, and the laser fluence reaching the target gradually decreases.

It was observed experimentally using 20 J/cm^2 fluence for 3, 4 and 5 pulses, the depth achieved is $3.6 \text{ }\mu\text{m}$, $4.3 \text{ }\mu\text{m}$ and $5.2 \text{ }\mu\text{m}$, respectively. From this data, it is inferred that for one pulse the depth is $\sim 1 \text{ }\mu\text{m}$. The depth achieved for 532 nm from the present model at 3000 K is thus validated with the experimental data. Figure 11(a) shows the temperature profile estimated using equation 1 for the 3 wavelengths for Cu sample. In the developed model, as we have not incorporated the effect of plasma and the change in

material properties with temperature, both 355 nm and 532 nm laser wavelengths follow the same trend, but since the reflectivity of 1064 nm for same fluence is high the temperature obtained at the surface is less than 355 nm and 532 nm. Figure 11(b) shows the variation of the recession rate with the depth for copper sample at different wavelengths. From the figure it could be observed that the trend of variation of recession rate is similar to that of the temperature. This observation is also proved experimentally with the depth results obtained for 1064 nm which is lesser compared to shorter wavelengths. Figure 12 shows the temperature profile for Al sample for 3 different wavelengths. The depth attained at boiling point temperature is less compared to Cu.

This developed model can be further improved by incorporating the effect of temperature on the material properties of the work piece and the plasma absorption phenomenon in order to predict the laser material interaction with more accuracy.

5. Conclusions

Influence of varying laser wavelengths namely 355 nm, 532 nm and 1064 nm on the characteristics of the micro channels generated during underwater scribing of metal thin films was studied. Greater depth for Al work piece was obtained in ablation in underwater medium than in air medium. As DI water level decreases, ablation rate becomes higher and the depth of channel increases. At DI water level, $h = 1 \text{ mm}$ depth of micro channel was maximum. With increase in DI water level the depth of the scribe channel reduces and this is attributed to the reduction in the plasma temperature due to quenching by excess water and thus reduction in the plasma pressure. With increase in energy of pulsed laser beam, the medium starts to break down due to parasitic breakdown at the interface of water and air and depth of micro channel remains unchanged at higher energies

Reflectivity of the work piece also results in the increased depth of the micro channels in underwater scribing due to multiple reflections of the shockwaves between the work-piece surface and the air-water interface. It was observed that shorter wavelength ablates more effectively compared to longer wavelength in DI water medium in case of Al, whereas for Cu, longer wavelength ablates more material in DI water medium compared to air. As energy increases, the width of channel also increases initially, but after 6 mJ of energy the change in width was limited to few microns. Melt pool was observed in dry (air) ablation and not in underwater ablation.

Acknowledgments

This work is partly supported by the grant-in aid from the Indian Space Research Organization (ISRO) (EDD/1415/151/ISRO/NILE).

The authors are grateful to the members of micro electronics and MEMS lab, Department of electrical engineering and physical metallurgy lab, Department of Metallurgical and Materials Engineering, IIT Madras for providing facilities for characterization.

References

- [1] M. J Jackson and W. O'Neill: *Journal of Materials Processing Technology*, 142, (2003) 517.
- [2] J.C Aurich, D. Dornfeld, P. J Arrazola, V. Franke, L. Leitz, and S. Min: *CIRP Annals-Manufacturing Technology*, 58, (2009) 519.
- [3] R. Fabbro, J. Fournier and P. Ballard, D. Devaux, J. Virmont: *Journals of Applied Physics*, 68, (1990) 775.
- [4] W. T. Chien, and S. C Hou.: *The International Journal of Advanced Manufacturing Technology*, 33, (2007) 308.
- [5] K. Hock, A. Benedikt, and R Hellmann: *Physics Procedia*, 39, (2012) p. 225.
- [6] N. Krstulović, S. Shannon, R. Stefanuik and C. Fanara: *The International Journal of Advanced Manufacturing Technology*, 69, (2013) 1765.
- [7] J Lu, R. Q. Xu, X. Chen, Z. H. Shen, X. W. Ni, S. Y. Zhang, and C. M. Gao: *Journal Of Applied Physics*, 95, (2004) 3890.
- [8] W. H. Kang, H. Lee, and A. J. Welch: *Journal of Applied Physics*, 103, (2008) 083101.
- [9] L. Tunna, A. Kearns, W. O'Neill, and C. J. Sutcliffe: *Optics & Laser Technology*, 33, (2001) 135-143.
- [10] S. Nammi, N. J. Vasa, G Balaganesan, S Gupta and A. C. Mathur: *Journal of Micro/Nanolithography, MEMS MOEMS*, 14, (2015) 044503.
- [11] J. J Chang, and B. E. Warner: *Applied physics letters*, 69, (1996) 473.
- [12] A. Bogaerts, C Zhaoyang, R Gijbels, and A.Vertes: *Atomic Spectroscopy*, 58, (2003) 1867.
- [13] A. Descoeurdes, C. Hollenstein, R. Demellayer, and G. Wälder: *Journal Of Materials Processing Technology*, 149, (2004) 184.
- [14] N. Aparna, N. J. Vasa, R. Sarathi, and J. Sundara Rajan: *Applied Physics A*, 117, (2014) 281.
- [15] J. M. Lee, C. Curran, K. G. Watkins: *Applied Physics A*, 73, (2001) 219.
- [16] D.W. Lynch, W.R. Hunter: "Handbook of Optical Constants of Solids" ed. by E.D. Palik, (Academic Press, 1985) p. 280.
- [17] L. Berthe, R. Fabbro, P. Peyre, L. Tollier, and E. Bartnicki: *Journals of Applied Physics*, 82, (1997) 2826.

(Received: May 26, 2015, Accepted: January 17, 2016)